


ORIGINAL RESEARCH

Identification of a 3-cuproptosis-associated-lncRNA-signature that predicts the prognosis of endometrial cancer patients

Tianyi Liu¹ , Xinyu Wang², Manyu Li³, Tianyu Zhu⁴, Cheng Qiu⁵, Chuhan He⁶, Lanyu Li⁷, Jinfeng Qu^{7,*}

¹Department of Medical Oncology, National Cancer Center/National Clinical Research Center for Cancer/Cancer Hospital, Chinese Academy of Medical Sciences and Peking Union Medical College, 100021 Beijing, China

²Department of Molecular Orthopaedics, National Center for Orthopaedics, Beijing Research Institute of Traumatology and Orthopaedics, Beijing Jishuitan Hospital, 100035 Beijing, China

³Cheeloo College of Medicine, Shandong University, 250012 Jinan, Shandong, China

⁴The Second Xiangya Hospital of Central South University, 410011 Changsha, Hunan, China

⁵Department of Orthopaedic Surgery, Qilu Hospital, Cheeloo College of Medicine, Shandong University, 250012 Jinan, Shandong, China

⁶The Second Hospital of Shandong University, Shandong University, 250033 Jinan, Shandong, China

⁷Department of Obstetrics and Gynecology, Central Hospital Affiliated to Shandong First Medical University, 250013 Jinan, Shandong, China

***Correspondence**

qjf2810@zxyy.cn
(Jinfeng Qu)

Abstract

Endometrial carcinoma is a common malignancy among peri-menopausal and menopausal females, even among some women of reproductive age. The treatment approach to endometrial cancer is a platinum-based regimen combined with paclitaxel, which may be unsatisfactory. A copper-mediated binding of lipoylated constituents of tricarboxylic acid cycle has been found recently, which brings about lethal protein stress and cell death, a phenomenon termed cuproptosis. As an innovative method of cell death, cuproptosis could be designed for cancer treatment and many aspects remain unaddressed. In our study, clinical, genomic, and mutational profiles of uterine corpus endometrial carcinoma (UCEC) patients were obtained from The Cancer Genome Atlas and cuproptosis-related genes and long non-coding RNAs (lncRNAs) were acquired thereafter. Co-expression and Cox regression analyses led to the development of a prognostic signature. Patients were separated into two groups (high- and low-risk groups) and survival analysis, risk score calculation, multivariate Cox analysis, and subgroup validation were implemented to determine the utility of the signature. Differentially expressed genes (DEGs) between the two groups were subjected to Gene Ontology and Kyoto Encyclopedia of Genes and Genomes enrichment analyses. Immune-related functional analysis and tumor mutation burden (TMB) analysis were performed. Three independent high-risk cuproptosis-related lncRNAs were finally confirmed and incorporated into the prognostic model, including BX322234.1, LINC01545 and LINC01224. Areas under the curve for 1-, 3- and 5-year survival were 0.717, 0.688 and 0.714, respectively. The risk model served as an independent factor to predict prognosis. Patients with high-risk and low TMB tended to have poor prognoses. Enrichment analysis demonstrated that DEGs were mostly associated with immune responses. In conclusion, the three high-risk cuproptosis-related lncRNAs could predict the prognosis of UCEC patients with higher power, where patients with high-risk and low TMB are prone to have the worst prognosis, which broadens the pattern of clinical treatment and applications.

Keywords

Cuproptosis; LncRNA; Endometrial carcinoma; Prognosis; LINC01224

1. Introduction

Endometrial carcinoma is a common malignancy among peri-menopausal and menopausal females, even among some women of reproductive age and accounts for the death of hundreds of thousands of women worldwide. Endometrial carcinoma reportedly causes approximately 76,000 deaths each year [1], and morbidity and mortality rates are still on the rise. Globally, over 410,000 new cases and nearly 100,000 deaths were reported in 2020 [2]. Endometrial carcinoma has been histologically classified into two types; one is the estrogen-dependent endometrioid adenocarcinoma, which is

connected with genetic alterations in kirsten rat sarcoma viral oncogene (*KRAS*), phosphatidylinositol-4,5-bisphosphate 3-kinase catalytic subunit alpha (*PIK3CA*), phosphatase and tensin homolog (*PTEN*), catenin beta 1 (*CTNNB1*) and mutL homolog 1 (*MLH1*) promoter hypermethylation, while the other is estrogen-independent serous adenocarcinoma, which, in contrast, prototypically harbors tumor protein p53 (*TP53*) mutations [3]. However, this dual classification has its limitation given the major molecular heterogeneity. Among treatment approaches, a platinum-based regimen in combination with paclitaxel is currently serving as the first-line treatment strategy for endometrial carcinoma patients,

which, nevertheless, has a low response rate and patients develop resistance soon after [3]. Therefore, considering that much remains to be addressed, there is an urgent need to elucidate the mechanisms underlying endometrial carcinoma to find alternative therapeutic methods.

In the past few years, great strides have been made in identifying several forms of programmed cell death (PCD) apart from classical apoptosis. Metal ions are fundamental micronutrients in the human body but some can induce PCD under certain conditions [4]. For example, ferroptosis is characterized as an iron (Fe)-dependent oxidative cell death induced by the accumulation of reactive oxygen species (ROS) and lipid peroxidation to lethal levels [5]. Moreover, a recent study reported that intracellular copper (Cu) induces a new type of PCD that varies from other forms of cell death involving apoptosis, necrocytosis, autophagy, ferroptosis, or pyroptosis, and is coined “cuproptosis” [6]. Specifically, mitochondrial stress, especially the recruitment of lipoylated enzymes in mitochondria and destabilization of iron-sulfur cluster proteins can evoke cuproptosis [4].

Cu participates in multitudes of biological processes as an essential trace element. Recent studies showed that, compared to healthy people, the level of Cu in cancer patients is markedly augmented in both peripheral blood and tumor tissues [7]. Although the imbalance in Cu homeostasis may induce cytotoxicity, changes in intracellular Cu levels may affect the malignant behavior, development, along with progression of tumors [8]. A Cu-mediated binding of lipoylated constituents of tricarboxylic acid cycle (TCA) has been found recently, giving rise to lethal protein stress and ultimately, cell death [6]. Cu ionophores comprising elesclomol, disulfiram, dithiocarbamates, *etc.*, together with Cu chelators including trientine, tetrathiomolybdate, *etc.* have been used as anticancer treating methods given the above mechanism [9].

2. Methods

2.1 Data collection, processing, and identification of cuproptosis-related long non-coding RNAs (lncRNAs)

The RNA-sequencing data of uterine corpus endometrial carcinoma (UCEC) patients were obtained from The Cancer Genome Atlas (TCGA) database (<https://portal.gdc.cancer.gov/>), with 554 tumor and 23 adjacent normal tissues in total. Clinical characteristics and mutations implicated in UCEC were downloaded as well, and lncRNAs were distinguished by the human gene annotations. Table 1 illustrates the clinicopathological features of these patients, and Table 2 shows the clinicopathological features of endometrioid endometrial adenocarcinoma patients from TCGA. Genes associated with cuproptosis were identified from previous publications [6, 10–13]. All the bioinformatic analyses were carried out using the R software (version 4.2.0, R Foundation for Statistical Computing, Vienna, Austria). An analysis of co-expression correlations between lncRNAs and cuproptosis-associated genes, performed with the limma package, identified lncRNAs that were related to cuproptosis ($|\text{Pearson } R| > 0.4, p < 0.001$) [14] and results were visualized

using the ggalluvial package.

TABLE 1. The clinical features of UCEC patients from TCGA.

Clinical feature	Type	Number
Status (%)		
	Alive	455 (83.5)
	Dead	90 (16.5)
Age		
	Mean (SD)	64 (11.1)
	Median (Min, Max)	64 (31, 90)
Race (%)		
	American Indian	4 (0.8)
	Asian	20 (3.9)
	Black	109 (21.1)
	Islander	9 (1.7)
	White	374 (72.5)
Grade (%)		
	G1	99 (18.1)
	G2	122 (22.3)
	G3	327 (59.7)
Histological type (%)		
	Endometrioid endometrial adenocarcinoma	411 (75.0)
	Mixed serous and endometrioid	22 (4.0)
	Serous endometrial adenocarcinoma	115 (21.0)
FIGO stage (%)		
	I	342 (62.4)
	II	52 (9.5)
	III	124 (22.6)
	IV	30 (5.5)

Note: SD, standard deviation; Min, minimum; Max, maximum; FIGO, The International Federation of Gynecology and Obstetrics.

2.2 Development of the cuproptosis-related lncRNA prognostic signature

Univariate Cox analysis was first conducted to identify putative lncRNAs associated with prognosis ($p < 0.001$). Next, a LASSO Cox regression analysis was conducted to further explore cuproptosis-related lncRNAs using a tenfold cross-validation method and establish a prognostic model. Thereafter, a multivariate Cox regression analysis was conducted to assess the efficacy of the constructed signature in predicting the prognosis of UCEC patients along with the clinicopathological characters. Risk scores were computed on the basis of LASSO regression analysis. The glmnet package was applied in R software [15].

TABLE 2. The clinical features of endometrioid endometrial adenocarcinoma patients from TCGA.

Clinical feature	Type	Number
Status (%)		
	Alive	360 (88.2)
	Dead	48 (11.8)
Age		
	Mean (SD)	62.5 (11.5)
	Median (Min, Max)	62 (31, 90)
Race (%)		
	American Indian	3 (0.8)
	Asian	17 (4.4)
	Black	69 (17.7)
	Islander	8 (2.1)
	White	293 (75.1)
Grade (%)		
	G1	98 (23.8)
	G2	120 (29.2)
	G3	193 (47.0)
FIGO stage (%)		
	I	290 (70.6)
	II	36 (8.8)
	III	71 (17.3)
	IV	14 (3.4)

Note: SD, standard deviation; Min, minimum; Max, maximum; FIGO, The International Federation of Gynecology and Obstetrics.

2.3 Analysis of risk score model, construction of nomogram and validation

In accordance with the median risk score, UCEC patients were separated into high- and low-risk groups. The pheatmap package was employed to plot the heatmap of the patient survival status in correlation with lncRNA expression dependent on risk scores. Kaplan-Meier (K-M) survival analysis was performed through the survival package to compare the overall survival (OS) and progression-free survival (PFS) for UCEC patients between the two groups. The survminer package was utilized to draw K-M curves. The prognostic value of risk score, as influenced by clinicopathological features including age and disease grade, was investigated using univariate and multivariate Cox analyses. The timeROC package was utilized to draw time-dependent receiver operating characteristic (ROC) curves to obtain the areas under curve (AUC) for 1-, 3- and 5-year survival predicted using the model [16]. C-index curves were drawn to confirm the model's efficacy.

Considering the clinical features, a predictive nomogram was developed using the Regression Modeling Strategies (rms) and survival packages to predict the survival rates for UCEC patients. The clinical information including age and disease grade was available and was included in the nomogram. For comparison of the model-predicted value against the actual outcomes, calibration curves were also plotted.

2.4 Principal component analysis (PCA) and functional enrichment analysis

PCA was conducted by means of the limma and scatterplot3d packages to visualize patients with different risk scores. Next, differentially expressed genes (DEGs) were distinguished between high- and low-risk groups by dint of the limma package, and genes with false discovery rate (FDR) < 0.05 and |log2 fold change (log2FC)| > 1 were considered statistically significant; thereafter the clusterProfiler package was used to conduct Gene Ontology (GO) and Kyoto Encyclopedia of Genes and Genomes (KEGG) enrichment analyses for DEGs; DEGs were classified into upregulated or downregulated genes depending on the positive and negative values of log2FC (a positive log2FC indicating upregulation while a negative log2FC indicating downregulation in high-risk patients) [17].

2.5 Immune-related functional analysis and tumor mutation burden (TMB) analysis

A comparison of immune-related functions between UCEC patients with distinguished risk levels was detected using the limma, Gene Set Variation Analysis (GSVA), and GSEABase packages, and $p < 0.05$ was considered statistically significant. Visualizing the differences was subsequently done with the pheatmap package. Then the limma, survival, and survminer packages were again utilized to conduct TMB analysis and plot the K-M curves between various groups of UCEC patients, while the ggpubr package was used to draw the violin plot of TMB differences.

2.6 Statistical analysis

All analyses were accomplished using the R software. Pearson correlation analysis was performed to filter cuproptosis-related lncRNAs. K-M curve analysis was conducted to make comparisons of the OS and PFS between diverse groups. Using univariate and multivariate Cox regression analyses, clinicopathological characteristics and risk scores were evaluated independently for prognosis. In our study, p -values were two-sided, and a p value < 0.05 was considered statistically significant unless otherwise specified.

3. Results

3.1 Identification of cuproptosis-related lncRNAs and development of the prognostic signature

After extracting the information on the expression of cuproptosis-related genes along with the lncRNAs in UCEC patients, and under the screening criteria of |Pearson R| > 0.4 and $p < 0.001$, 1285 lncRNAs related to cuproptosis

were filtered from a total of 16,876 lncRNAs. The Sankey diagram illustrated the co-expression between cuproptosis-related genes and lncRNAs (Fig. 1A). UCEC patients were evenly divided into two groups at random, *i.e.*, the training group and the test group. In the training group, four prognostic lncRNAs (BX322234.1, LINC01545, LINC01936 and LINC01224) were initially identified by univariate Cox regression (Fig. 1B), which were further verified by LASSO Cox regression (Fig. 1C and D) and multivariate Cox regression with three remaining lncRNAs obtained as independent prognostic factors. A risk score for UCEC patients was derived from expression of BX322234.1, LINC01545 and LINC01224 using the formula below: Risk score = $(0.686683153567569 \times \text{BX322234.1}) + (0.558196515747439 \times \text{LINC01545}) + (0.180619223395381 \times \text{LINC01224})$. A heatmap exhibiting the relationship between cuproptosis-related genes and lncRNAs is shown in Fig. 1E.

3.2 Survival analysis of different groups

Patients in the training group were categorized into high- and low-risk subgroups in accordance with the median risk score, which served as the cutoff value. Likewise, patients in the test group were separated into two groups using the same cutoff value and so were all the patients (Fig. 2A–C). High-risk patients in both training and test groups showed a high expression of BX322234.1, LINC01545 and LINC01224 while those at low-risk had corresponding low expression (Fig. 2D–F), suggesting that BX322234.1, LINC01545 and LINC01224 were high-risk lncRNAs for UCEC patients. As shown in the scatter diagrams (Fig. 2G–I), high-risk patients tended to have an unfavorable prognosis, *i.e.*, a shorter OS, which is also demonstrated in the K-M curves (Fig. 2J–L). Worse still, a shorter PFS was observed (Fig. 3A).

3.3 Independent prognostic analysis of the signature

Univariate and multivariate Cox regression analyses were conducted to validate whether the risk score depending on the three-lncRNA-signature we developed, could be utilized as a prognostic factor independent of other clinical features. Although all three factors, namely age, grade, and risk score showed statistical significance in the univariate Cox analysis (Fig. 3B), judging from the conclusion of multivariate Cox analysis, only grade and risk score could predict the prognosis of UCEC patients independently with corresponding *p* values of < 0.001 (hazard ratio (HR) = 2.239; 95% confidence interval (CI), 1.469–3.413) and 0.007 (HR = 1.200; 95% CI, 1.051–1.370) (Fig. 3C). Since we plotted the C-index curve, the risk score was found to be best at predicting prognosis than the other two factors (Fig. 3D). Moreover, ROC curves for 1-year survival showed that AUC for the risk score was 0.717, ranking the first among the three factors (age, 0.594; grade, 0.650) (Fig. 3E). The AUC for 1-, 3- and 5-year survival were 0.717, 0.688 and 0.714, respectively, reconfirming the prognosis-predictive role of the risk score (Fig. 3F).

3.4 Construction of the nomogram and validation in different groups

A predictive nomogram was drawn using age, grade, and risk and an example was plotted to show the probability of 1-, 3- and 5-year survival of a patient with a score of 114 (Fig. 4A). Calibration curves were used to demonstrate the prediction model's accuracy (Fig. 4B). Next, the prediction model was further verified for UCEC patients of different grades. The K-M curves showed that the prediction model could be used for distinguishing patients with different disease grades (Fig. 4C–E), indicating that the model not only had a high accuracy of prediction but also could be applied to patients with different backgrounds.

3.5 Immune-related functional analysis and TMB analysis

Immune-related functional analysis was performed between high- and low-risk groups to reveal the role of immune status in UCEC progression in addition to predicting the prognosis. As shown in the heatmap, 11 out of the 13 immune-related functions, involving interferon (IFN) response (both type 1 and 2), cytolytic activity, inflammation promoting, checkpoint, T cell co-inhibition, antigen-presenting cell (APC) co-stimulation, C-C motif chemokine receptor (CCR), T cell co-stimulation, human leukocyte antigen (HLA), and APC co-inhibition differed significantly between two groups (Fig. 4F). Among the 11 immune-associated functions, type 1 IFN response was significantly upregulated in the high-risk group while the left was downregulated, implying that IFN played a vital role in UCEC. Furthermore, we explored the discrepancy in TMB between the two groups and found that low-risk patients had a higher TMB (Fig. 4G) which correlated with a better prognosis (Fig. 5A). Considering the TMB and risk, we concluded that high-risk patients with a low TMB had the poorest clinical outcomes (Fig. 5B).

3.6 PCA and functional enrichment analysis

All genes (Fig. 5C), cuproptosis-related genes (Fig. 5D), cuproptosis-related lncRNAs (Fig. 5E), and risk lncRNAs (Fig. 5F) were considered in the PCA analysis of patient distribution. We observed that risk lncRNAs (Fig. 5F), along with all genes (Fig. 5C), were obviously discriminated between high- and low-risk groups, while the cuproptosis-related genes and lncRNAs were slightly tangled between the two groups despite a visible trend. GO analysis showed that the upregulated risk DEGs in the high-risk group were mostly enriched in axon development, axonogenesis, and synapse organization (Fig. 5G) and downregulated risk DEGs were mostly enriched in immunoglobulin complex (Fig. 5H). KEGG results exhibited that upregulated risk DEGs were enriched in the neuroactive ligand-receptor interaction pathway (Fig. 5I) and the downregulated risk DEGs were prominently enriched in the interleukin 17 signaling pathway (Fig. 5J).

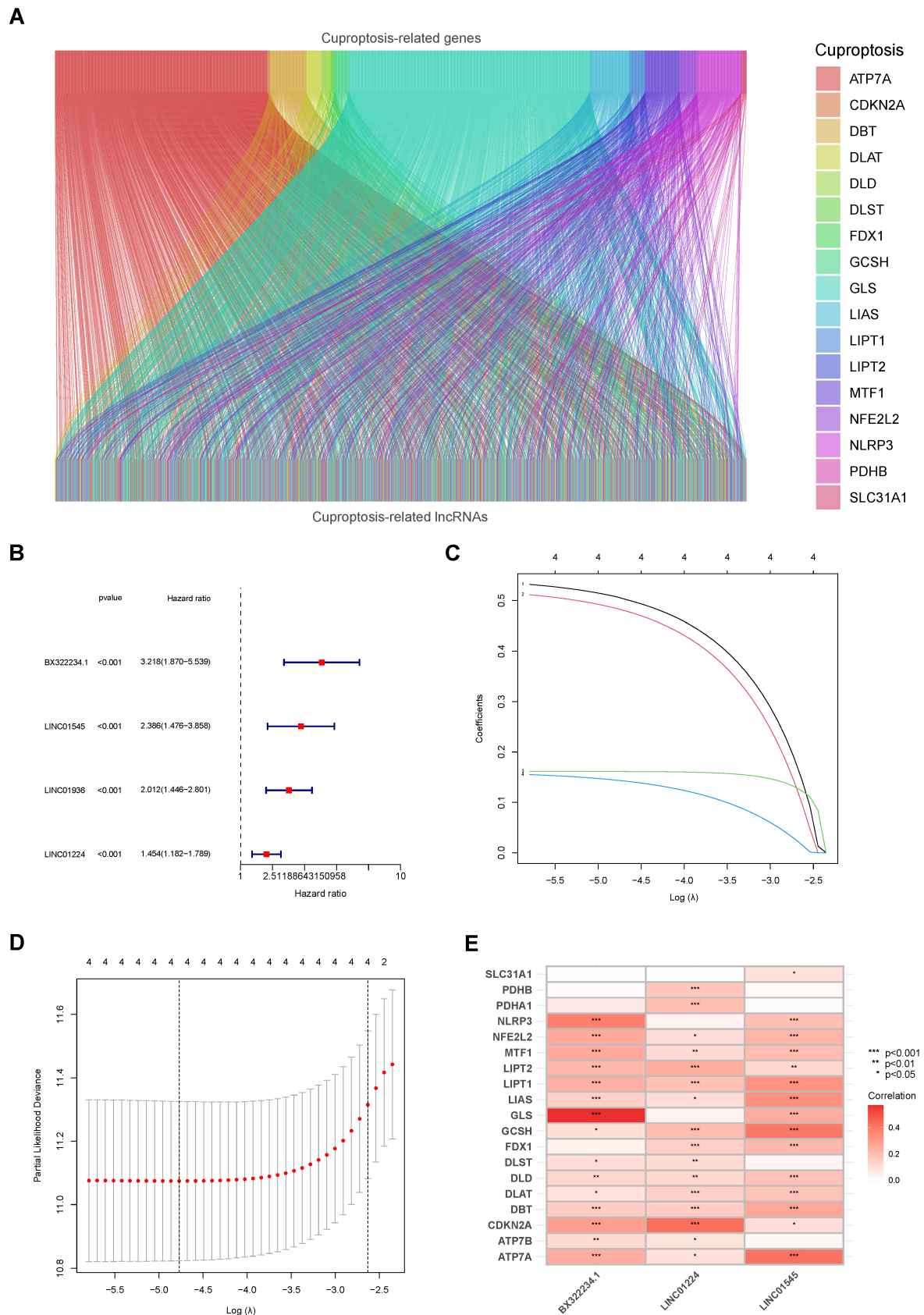
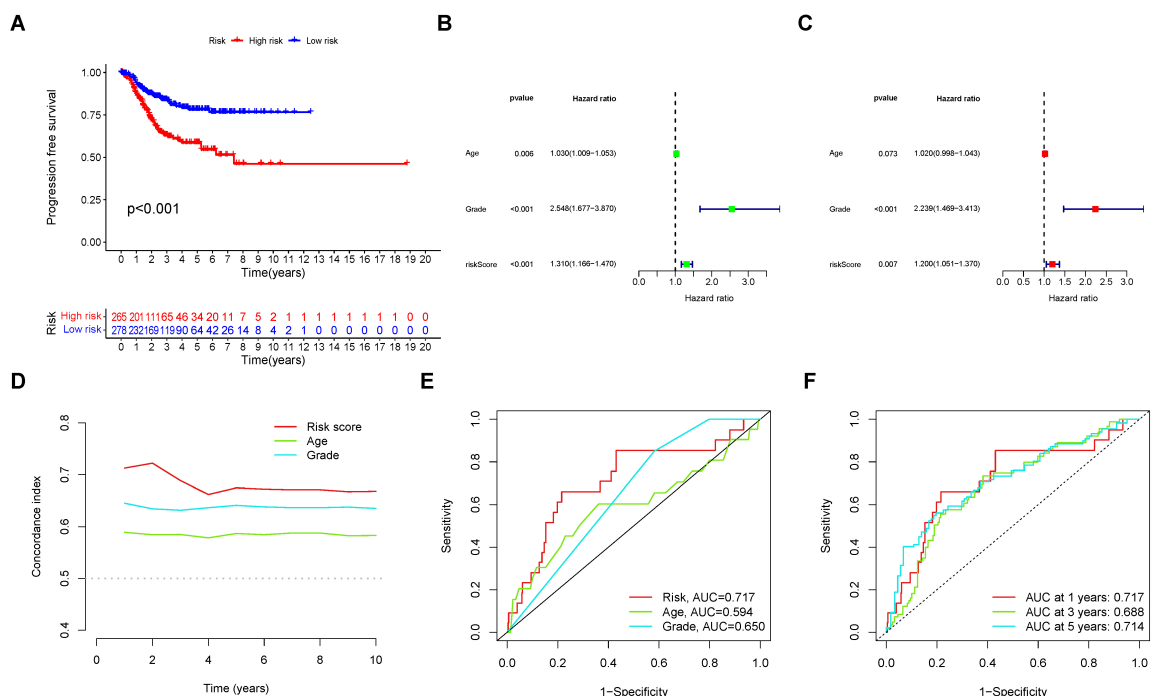
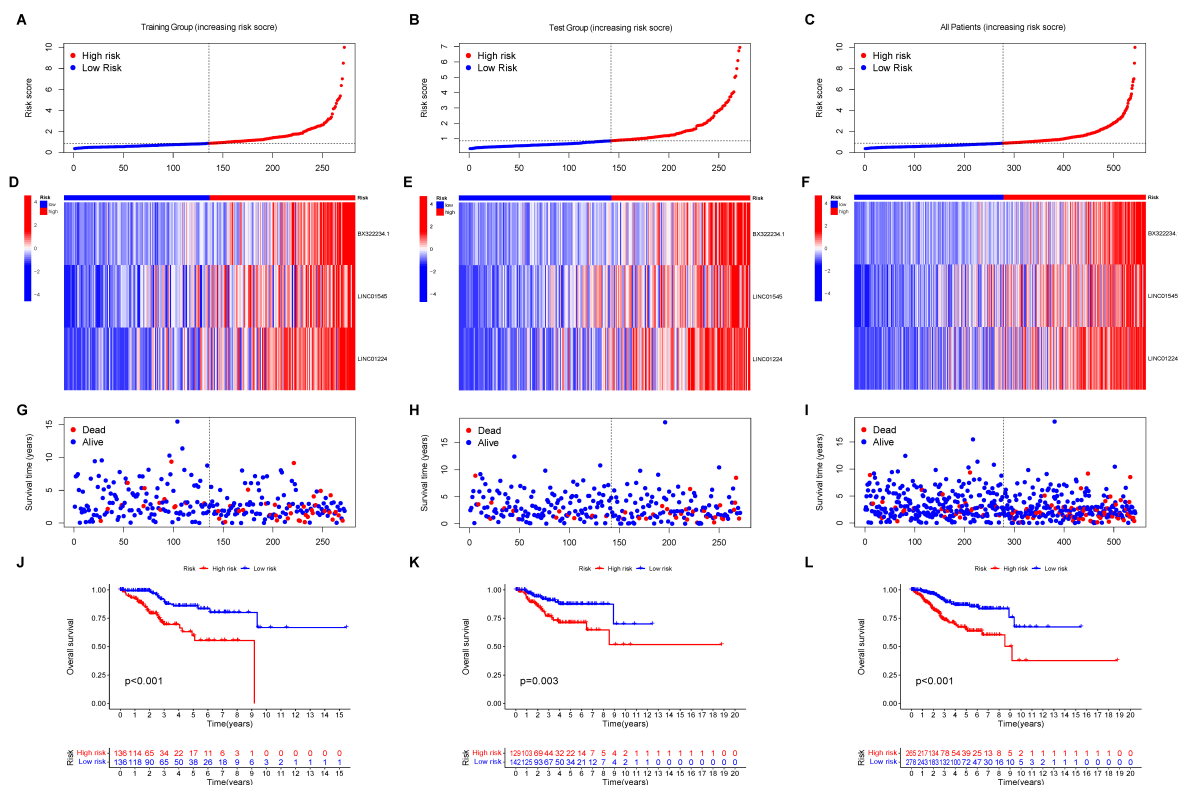


FIGURE 1. Screening of candidate cuproptosis-related lncRNAs with prognostic value. (A) Sankey diagram of co-expression between cuproptosis-related genes and lncRNAs. Seventeen cuproptosis-related genes are screened out in total. (B) Forest plot of univariate Cox analysis of four candidate prognostic lncRNAs. (C, D) LASSO Cox regression analysis of prognostic lncRNAs. (E) The correlations between nineteen cuproptosis-related genes and three independent prognostic lncRNAs. * $p < 0.05$; ** $p < 0.01$; *** $p < 0.001$.



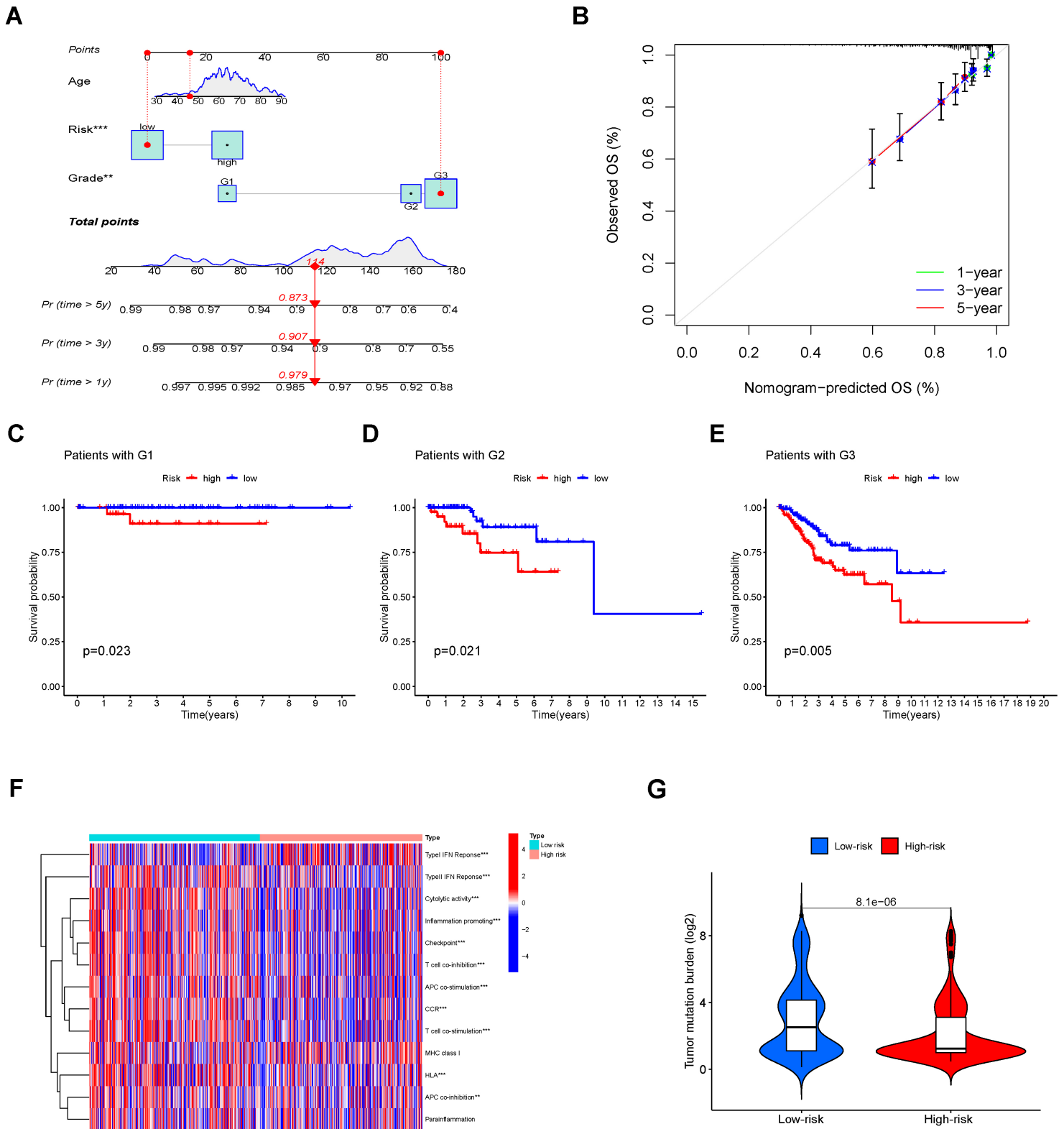


FIGURE 4. Construction of the prognostic nomogram and related analyses. (A) The nomogram based on age, grade and risk predicts the probability of 1-, 3- and 5-year survival and an example of a patient with a point of 114. (B) Calibration curves of the difference between the model-predicted value against the actual outcomes. (C–E) Kaplan-Meier survival curves of survival probability in high- and low-risk patients with different disease grades. (F) The heatmap of differences of thirteen immune-related functions between high- and low-risk groups. (G) The violin plot of differences of TMB between patients with different risks. Note: Pr, predicted; 5 y, 5 years; 3 y, 3 years; 1 y, 1 year; G1: Grade 1; G2: Grade 2; G3: Grade 3; OS, overall survival. ** $p < 0.01$; *** $p < 0.001$.

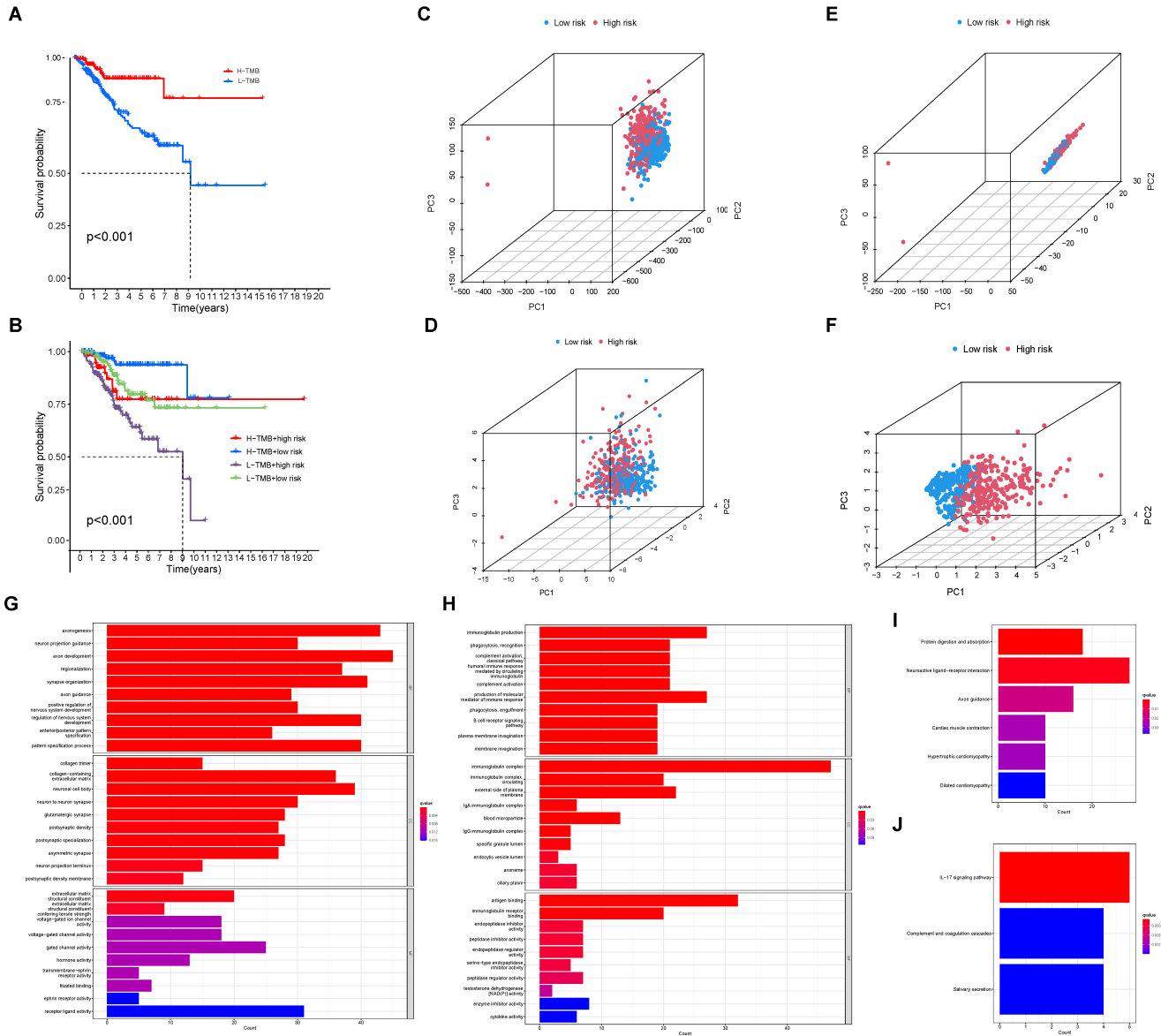


FIGURE 5. Kaplan-Meier, PCA and functional enrichment analyses. (A) Kaplan-Meier survival curves of patients with different TMB. (B) Kaplan-Meier survival curves of patients with different combinations of TMB and risks. (C) All genes, (D) cuproptosis-related genes, (E) cuproptosis-related lncRNAs, and (F) risk lncRNAs in the PCA analysis of patient distribution. (G, H) The GO enrichment analyses of upregulated and downregulated DEGs in high-risk patients. (I, J) The KEGG pathway enrichment analyses of upregulated and downregulated DEGs in high-risk patients. Note: TMB, tumor mutation burden; GO: Gene Ontology; BP, biological process; CC, cellular component; MF, molecular function; KEGG, Kyoto Encyclopedia of Genes and Genomes.

4. Discussion

As an essential micronutrient, Cu plays an important role in maintaining normal physiological functions with the assistance of various carrier proteins and metabolic enzymes [18]. When the metabolism of Cu is hindered, some diseases including Wilson disease [19], Menkes disease [20], and cancers [21] emerge. In terms of the relationship between Cu and cancer, higher Cu concentrations have been found in both tumor tissues and sera of cancer patients [22–24], which may be the result of the activation of cell proliferation-related pathways. Therefore, there have been two main Cu-targeted therapeutic strategies, *i.e.*, using Cu chelators and Cu ionophores along with the radioisotope ^{64}Cu for both imaging and therapy [21,

25]. Based on these studies, scientists recently discovered a PCD closely related to Cu and termed it cuproptosis.

Cuproptosis, similar to ferroptosis [26], is defined as cell death induced by Cu toxicity due to its accumulation. Unlike other forms of PCD, cuproptosis participates in mitochondrial cell death by regulating the TCA cycle. Experiments showed that blocking any known PCD pathway could not inhibit Cu-induced death, thus fully manifesting its novelty [6]. Since its discovery, several studies have explored its connection with tumors, including in breast cancer [27, 28], bladder cancer [29, 30], hepatocellular carcinoma [31, 32], renal cell carcinoma [33, 34], pancreatic carcinoma [35, 36], and lung cancer [37, 38]. Existing research has mainly focused on the cuproptosis-related tumor microenvironment, cuproptosis-related lncRNA,

and their value in predicting therapeutic effects and prognosis. In this study, expression data of lncRNAs of UCEC patients were collected from a public database. Through Pearson correlation analysis, cuproptosis-related lncRNAs were screened, and the co-expression of cuproptosis-related lncRNAs and genes was analyzed. Then, multivariate Cox regression analysis filtered three independent prognostic cuproptosis-related lncRNAs, namely BX322234.1, LINC01224 and LINC01545.

LncRNA BX322234.1 was first reported as an autophagy-related lncRNA in UCEC, and its high expression level was related to worse survival condition [39]. In another study, BX322234.1 was screened in a genomic instability-derived lncRNA signature [40]. Thus, both the previous studies and our findings confirmed the prognostic value of BX322234.1 in UCEC patients but its functions other than predicting the prognosis, including involvement in tumor progression, warrant further investigation.

LncRNA LINC01224 was first screened as a *BRCA*-related differentially expressed lncRNA [41]. It was found to be connected to breast cancer [41], hepatocellular carcinoma [42], malignant melanoma [43], and esophageal squamous cell carcinoma [44]. Mostly, LINC01224 is thought to be diagnostic and prognostic as its high level may indicate a higher risk and worse prognosis. Moreover, the downregulation of LINC01224 helps delay tumorigenesis and promotes apoptosis. A study proved its mechanism of action, whereby Yin Yang 1, a well-acknowledged transcription factor for lncRNAs, induces LINC01224 expression which further regulates cancer progression by mediating the crosstalk between miR-485-5p and Myosins of class VI (MYO6) [45], sponging miR-2467 [46], sponging miR-6884-5p to activate the Wnt/ β -catenin pathway [44], regulating miR-193a-5p and cyclin-dependent kinase 8 (CDK8) [47], and promoting the expression of nuclear receptor subfamily 1 group D member 2 (NR1D2) [43]. In UCEC, LINC01224 was found to promote the progression by mediating the miR-485-5p/AKT3 axis [48] and its high level also suggests a worse prognosis [49]. Apart from regulating apoptosis during tumorigenesis, a study found that LINC01224 participates in ferroptosis [50], an iron-induced PCD type, and along with its relation to cuproptosis, this highlights the potential of further study on the relationship between LINC01224 and cuproptosis. However, the functions or mechanistic details of LINC01545 action have never been reported before and need to be explored.

The three cuproptosis-related lncRNAs we identified, especially LINC01224, have been reported to exert a significant influence on the development of certain cancers, and therefore may be used as a therapeutic target for the development of corresponding drugs in the future. In contrast, LINC01545 has not been reported in previous studies, which implies that this might be a new potential target for the treatment of UCEC and its biological roles in UCEC will be the priorities of future studies. In addition, the prognosis model constructed in this study has good predictive power and stability as an independent predictor and prognostic biomarker for UCEC and outperforms other clinical factors. The relationship between risk score and survival time for all patients suggested that patients in the high-risk group might have significantly shorter PFS and OS compared to their low-risk counterparts. Accordingly, during

clinical diagnosis and treatment process, for UCEC patients with complete clinicopathological information who underwent RNA-seq testing, our nomogram could be used for clinical guidance to predict prognosis and also to evaluate treatment efficacy.

Nevertheless, our research still has some limitations that warrant consideration. Since cuproptosis is a newly discovered PCD type, the detailed and relevant mechanism has not been fully elucidated. Our work lacks experimental verification. Therefore, further investigations into its underlying mechanisms are needed.

In summary, our study revealed that three independent prognostic cuproptosis-related lncRNAs, namely BX322234.1, LINC01224 and LINC01545, play a pivotal role in the prognosis of UCEC and suggested that cuproptosis might participate in the development of UCEC, which could help clinicians gain a new understanding of the potential mechanisms of UCEC and find new ways of treating UCEC by exploiting Cu metabolism-related regulatory mechanisms. In addition, we developed a prognostic model along with the age, risk score, and grade for predicting the survival of UCEC patients during three different time periods with promising predictive power, and analyzed the immune-related functions and TMB of UCEC patients, which may help the clinicians to predict the prognosis of different UCEC patients and combine different roles of cuproptosis across UCEC patients for individualized treatment.

5. Conclusions

In this study, we developed a cuproptosis-related lncRNA signature for UCEC patients, constructed a nomogram, and analyzed immune-related functions, functional and pathway enrichment analyses, and TMB in combination with risks in UCEC patients. Our study could support ideas for clinicians in analyzing risk for UCEC patients, provide novel insight into the prediction of prognosis of UCEC patients, as well as offer some evidence for further research on cuproptosis-related mechanisms underlying cancer cell death.

AVAILABILITY OF DATA AND MATERIALS

The raw data supporting the conclusion of this article will be made available by the authors, without undue reservation.

AUTHOR CONTRIBUTIONS

TYL—Conceptualization, Data curation, Formal analysis, Methodology, Software, Validation, Visualization; TYL, XYW—Investigation; TYL, XYW, MYL—Writing-original draft; TYL, XYW, MYL, TYZ, CQ, CHH, JFQ—Writing-review & editing; LYL, JFQ—Project administration; Resources; JFQ—Supervision. All authors read and approved the final manuscript.

ETHICS APPROVAL AND CONSENT TO PARTICIPATE

Not applicable.

ACKNOWLEDGMENT

Not applicable.

FUNDING

This research received no external funding.

CONFLICT OF INTEREST

The authors declare no conflict of interest.

REFERENCES

- [1] Siegel RL, Miller KD, Fuchs HE, Jemal A. Cancer statistics, 2021. *CA: A Cancer Journal for Clinicians*. 2021; 71: 7–33.
- [2] Sung H, Ferlay J, Siegel RL, Laversanne M, Soerjomataram I, Jemal A, *et al*. Global cancer statistics 2020: GLOBOCAN estimates of incidence and mortality worldwide for 36 cancers in 185 countries. *CA: A Cancer Journal for Clinicians*. 2021; 71: 209–249.
- [3] Colombo N, Creutzberg C, Amant F, Bosse T, González-Martín A, Ledermann J, *et al*. ESMO-ESGO-ESTRO consensus conference on endometrial cancer: diagnosis, treatment and follow-up. *Radiotherapy and Oncology*. 2015; 117: 559–581.
- [4] Tang D, Chen X, Kroemer G. Cuproptosis: a copper-triggered modality of mitochondrial cell death. *Cell Research*. 2022; 32: 417–418.
- [5] Chen X, Kang R, Kroemer G, Tang D. Broadening horizons: the role of ferroptosis in cancer. *Nature Reviews Clinical Oncology*. 2021; 18: 280–296.
- [6] Tsvetkov P, Coy S, Petrova B, Dreishpoon M, Verma A, Abdusamad M, *et al*. Copper induces cell death by targeting lipoylated TCA cycle proteins. *Science*. 2022; 375: 1254–1261.
- [7] Ge EJ, Bush AI, Casini A, Cobine PA, Cross JR, DeNicola GM, *et al*. Connecting copper and cancer: from transition metal signalling to metalloplasia. *Nature Reviews Cancer*. 2022; 22: 102–113.
- [8] Babak MV, Ahn D. Modulation of intracellular copper levels as the mechanism of action of anticancer copper complexes: clinical relevance. *Biomedicine*. 2021; 9: 852.
- [9] Davis CI, Gu X, Kiefer RM, Ralle M, Gade TP, Brady DC. Altered copper homeostasis underlies sensitivity of hepatocellular carcinoma to copper chelation. *Metallomics*. 2020; 12: 1995–2008.
- [10] Polishchuk EV, Merolla A, Lichtmannegger J, Romano A, Indrieri A, Ilyechova EY, *et al*. Activation of autophagy, observed in liver tissues from patients with wilson disease and from ATP7B-deficient animals, protects hepatocytes from copper-induced apoptosis. *Gastroenterology*. 2019; 156: 1173–1189.e5.
- [11] Aubert L, Nandagopal N, Steinhart Z, Lavoie G, Nourredine S, Berman J, *et al*. Copper bioavailability is a KRAS-specific vulnerability in colorectal cancer. *Nature Communications*. 2020; 11: 3701.
- [12] Dong J, Wang X, Xu C, Gao M, Wang S, Zhang J, *et al*. Inhibiting NLRP3 inflammasome activation prevents copper-induced neuropathology in a murine model of Wilson's disease. *Cell Death & Disease*. 2021; 12: 87.
- [13] Ren X, Li Y, Zhou Y, Hu W, Yang C, Jing Q, *et al*. Overcoming the compensatory elevation of NRF2 renders hepatocellular carcinoma cells more vulnerable to disulfiram/copper-induced ferroptosis. *Redox Biology*. 2021; 46: 102122.
- [14] Ritchie ME, Phipson B, Wu D, Hu Y, Law CW, Shi W, *et al*. Limma powers differential expression analyses for RNA-sequencing and microarray studies. *Nucleic Acids Research*. 2015; 43: e47.
- [15] Friedman J, Hastie T, Tibshirani R. Regularization paths for generalized linear models via coordinate descent. *Journal of Statistical Software*. 2010; 33: 1–22.
- [16] Blanche P, Dartigues J, Jacqmin-Gadda H. Estimating and comparing time-dependent areas under receiver operating characteristic curves for censored event times with competing risks. *Statistics in Medicine*. 2013; 32: 5381–5397.
- [17] Wu T, Hu E, Xu S, Chen M, Guo P, Dai Z, *et al*. ClusterProfiler 4.0: a universal enrichment tool for interpreting omics data. *The Innovation*. 2021; 2: 100141.
- [18] Jomova K, Makova M, Alomar SY, Alwasel SH, Nepovimova E, Kuca K, *et al*. Essential metals in health and disease. *Chemico-Biological Interactions*. 2022; 367: 110173.
- [19] Czlönkowska A, Litwin T, Dusek P, Ferenci P, Lutsenko S, Medici V, *et al*. Wilson disease. *Nature Reviews Disease Primers*. 2018; 4: 21.
- [20] Guthrie LM, Soma S, Yuan S, Silva A, Zulkifli M, Snavelly TC, *et al*. Elesclomol alleviates Menkes pathology and mortality by escorting Cu to cuproenzymes in mice. *Science*. 2020; 368: 620–625.
- [21] Ge EJ, Bush AI, Casini A, Cobine PA, Cross JR, DeNicola GM, *et al*. Connecting copper and cancer: from transition metal signalling to metalloplasia. *Nature Reviews Cancer*. 2022; 22: 102–113.
- [22] Feng Y, Zeng J, Ma Q, Zhang S, Tang J, Feng J. Serum copper and zinc levels in breast cancer: a meta-analysis. *Journal of Trace Elements in Medicine and Biology*. 2020; 62: 126629.
- [23] Saleh SAK, Adly HM, Abdelkhalik AA, Nassir AM. Serum levels of selenium, zinc, copper, manganese, and iron in prostate cancer patients. *Current Urology*. 2020; 14: 44–49.
- [24] Wach S, Weigelt K, Michalke B, Lieb V, Stoeck R, Keck B, *et al*. Diagnostic potential of major and trace elements in the serum of bladder cancer patients. *Journal of Trace Elements in Medicine and Biology*. 2018; 46: 150–155.
- [25] Lopez J, Ramchandani D, Vahdat L. Copper depletion as a therapeutic strategy in cancer. *Metal Ions in Life Sciences*. 2019; 19: 303–330.
- [26] Jiang X, Stockwell BR, Conrad M. Ferroptosis: mechanisms, biology and role in disease. *Nature Reviews Molecular Cell Biology*. 2021; 22: 266–282.
- [27] Sha S, Si L, Wu X, Chen Y, Xiong H, Xu Y, *et al*. Prognostic analysis of cuproptosis-related gene in triple-negative breast cancer. *Frontiers in Immunology*. 2022; 13: 922780.
- [28] Li Z, Zhang H, Wang X, Wang Q, Xue J, Shi Y, *et al*. Identification of cuproptosis-related subtypes, characterization of tumor microenvironment infiltration, and development of a prognosis model in breast cancer. *Frontiers in Immunology*. 2022; 13: 996836.
- [29] Song Q, Zhou R, Shu F, Fu W. Cuproptosis scoring system to predict the clinical outcome and immune response in bladder cancer. *Frontiers in Immunology*. 2022; 13: 958368.
- [30] Bai Y, Zhang Q, Liu F, Quan J. A novel cuproptosis-related lncRNA signature predicts the prognosis and immune landscape in bladder cancer. *Frontiers in Immunology*. 2022; 13: 1027449.
- [31] Ding L, Li W, Tu J, Cao Z, Li J, Cao H, *et al*. Identification of cuproptosis-related subtypes, cuproptosis-related gene prognostic index in hepatocellular carcinoma. *Frontiers in Immunology*. 2022; 13: 989156.
- [32] Yan C, Niu Y, Ma L, Tian L, Ma J. System analysis based on the cuproptosis-related genes identifies LIPT1 as a novel therapy target for liver hepatocellular carcinoma. *Journal of Translational Medicine*. 2022; 20: 452.
- [33] Wang T, Liu Y, Li Q, Luo Y, Liu D, Li B. Cuproptosis-related gene FDX1 expression correlates with the prognosis and tumor immune microenvironment in clear cell renal cell carcinoma. *Frontiers in Immunology*. 2022; 13: 999823.
- [34] Pang Y, Wang Y, Zhou X, Ni Z, Chen W, Liu Y, *et al*. Cuproptosis-Related lncRNA-based prediction of the prognosis and immunotherapy response in papillary renal cell carcinoma. *International Journal of Molecular Sciences*. 2023; 24: 1464.
- [35] Huang X, Zhou S, Tóth J, Hajdu A. Cuproptosis-related gene index: a predictor for pancreatic cancer prognosis, immunotherapy efficacy, and chemosensitivity. *Frontiers in Immunology*. 2022; 13: 978865.
- [36] Liu Q, Li R, Wu H, Liang Z. A novel cuproptosis-related gene model predicts outcomes and treatment responses in pancreatic adenocarcinoma. *BMC Cancer*. 2023; 23: 226.
- [37] Wang S, Xing N, Meng X, Xiang L, Zhang Y. Comprehensive bioinformatics analysis to identify a novel cuproptosis-related prognostic

- signature and its ceRNA regulatory axis and candidate traditional Chinese medicine active ingredients in lung adenocarcinoma. *Frontiers in Pharmacology*. 2022; 13: 971867.
- [38] Chen Y, Tang L, Huang W, Zhang Y, Abisola FH, Li L. Identification and validation of a novel cuproptosis-related signature as a prognostic model for lung adenocarcinoma. *Frontiers in Endocrinology*. 2022; 13: 963220.
- [39] Wang X, Dai C, Ye M, Wang J, Lin W, Li R. Prognostic value of an autophagy-related long-noncoding-RNA signature for endometrial cancer. *Aging*. 2021; 13: 5104–5119.
- [40] Huo X, Wang S, Yang Q, Yu X, Gu T, Hua H, *et al.* Diagnostic and prognostic value of genomic instability-derived long non-coding RNA signature of endometrial cancer. *Taiwanese Journal of Obstetrics and Gynecology*. 2022; 61: 96–101.
- [41] Li H, Gao C, Liu L, Zhuang J, Yang J, Liu C, *et al.* 7-lncRNA assessment model for monitoring and prognosis of breast cancer patients: based on cox regression and co-expression analysis. *Frontiers in Oncology*. 2019; 9: 1348.
- [42] Gong A, Luo X, Tan Y, Chen H, Luo G. High expression of C10orf91 and LINC01224 in hepatocellular carcinoma and poor prognosis. *American Journal of Translational Research*. 2022; 14: 2567–2579.
- [43] Cui Y, Zheng Y, Lu Y, Zhang M, Yang L, Li W. LINC01224 facilitates the proliferation and inhibits the radiosensitivity of melanoma cells through the miR-193a-5p/NR1D2 axis. *The Kaohsiung Journal of Medical Sciences*. 2022; 38: 196–206.
- [44] Qiang G, Yu Q, Su K, Guo Y, Liu D, Liang C. E2F1-activated LINC01224 drives esophageal squamous cell carcinoma cell malignant behaviors *via* targeting miR-6884-5p/DVL3 axis and activating Wnt/ β -catenin signaling pathway. *Pathology—Research and Practice*. 2022; 235: 153873.
- [45] Gu J, Dong L, Wang Y, Nie W, Liu W, Zhao J. LINC01224 promotes colorectal cancer progression through targeting miR-485-5p/MYO6 axis. *World Journal of Surgical Oncology*. 2021; 19: 281.
- [46] Xiao S, Sun L, Ruan B, Li J, Chen J, Xiong J, *et al.* Long non-coding RNA LINC01224 promotes progression and cisplatin resistance in non-small lung cancer by sponging miR-2467. *Pulmonary Pharmacology & Therapeutics*. 2021; 70: 102070.
- [47] Sun H, Yan J, Tian G, Chen X, Song W. LINC01224 accelerates malignant transformation *via* MiR-193a-5p/CDK8 axis in gastric cancer. *Cancer Medicine*. 2021; 10: 1377–1393.
- [48] Zuo X, Li W, Yan X, Ma T, Ren Y, Hua M, *et al.* Long non-coding RNA LINC01224 promotes cell proliferation and inhibits apoptosis by regulating AKT3 expression *via* targeting miR-485-5p in endometrial carcinoma. *Oncology Reports*. 2021; 46: 186.
- [49] Xu H, Zou R, Liu J, Zhu L. A risk signature with nine stemness index-associated genes for predicting survival of patients with uterine corpus endometrial carcinoma. *Journal of Oncology*. 2021; 2021: 1–17.
- [50] Xu Z, Peng B, Liang Q, Chen X, Cai Y, Zeng S, *et al.* Construction of a ferroptosis-related nine-lncRNA signature for predicting prognosis and immune response in hepatocellular carcinoma. *Frontiers in Immunology*. 2021; 12: 719175.

How to cite this article: Tianyi Liu, Xinyu Wang, Manyu Li, Tianyu Zhu, Cheng Qiu, Chuhan He, *et al.* Identification of a 3-cuproptosis-associated-lncRNA-signature that predicts the prognosis of endometrial cancer patients. *European Journal of Gynaecological Oncology*. 2023. doi: 10.22514/ejgo.2023.073.